Building and Environment 244 (2023) 110763

Contents lists available at ScienceDirect

Building and Environment

journal homepage: www.elsevier.com/locate/buildenv

Size-resolved inhalation intake fractions for particles released from human activities in residential indoor environments

Dusan Licina [a,*], Brandon E. Boor [b,c]

[a] Human-Oriented Built Environment Lab, School of Architecture, Civil and Environmental Engineering, École Polytechnique Fédérale de Lausanne (EPFL), Switzerland
[b] Lyles School of Civil Engineering, Purdue University, West Lafayette, IN, USA
[c] Ray W. Herrick Laboratories, Center for High Performance Buildings, Purdue University, West Lafayette, IN, USA

ARTICLE INFO

Keywords:
Personal exposure
Indoor aerosols
Spatial uniformity
Human occupancy
Emissions

ABSTRACT

Inhalation exposure to elevated concentrations of airborne particulate matter is a public health concern. Assessment of exposure can be enhanced through better knowledge of source-receptor relationships, which can be characterized through the inhalation intake fraction metric. This case study provides new insights on variations in particle inhalation intake fractions for indoor sources associated with common human activities in residential buildings. In a controlled climate chamber (air temperature: 24 ± 1 °C, relative humidity: 50 ± 5%), we investigated size-resolved intake fractions for particles in relation to four scripted activities performed by a human volunteer: sitting, walking, cooking, and vacuuming. We measured size- and time-resolved particle number concentrations at the volunteer's breathing zone to characterize intake fractions. In addition, we measured particles at four different stationary locations across the climate chamber to assess the degree of spatial heterogeneity in particulate matter concentrations. The results show that particles released from human skin and clothing during sitting were associated with the highest total inhalation intake fraction (13‰), followed by cooking (9‰), vacuuming (5.7‰), and walking (3.9‰). These results highlight how breathing zone proximity to localized emission sources and low indoor air mixing can enhance inhalation exposure to particles. Sitting and cooking caused a maximum inhalation intake fraction in the size range of 1–3 μm. Findings also show that the assumption of a perfectly mixed environment could lead to an underestimation of the inhalation intake of particles by up to 3.2-fold. The results of this case study provide a basis for achieving more accurate personal inhalation exposure assessment and improved indoor air quality management.

1. Introduction

Inhalation exposure to elevated concentrations of coarse (≤10 μm) and fine (≤2.5 μm) airborne particulate matter (PM) is a major environmental health challenge that is associated with an increase in morbidity and mortality [1–3]. Personal exposure to particles in enclosed environments is especially important as people spend the majority of their time indoors [4,5]. As modern buildings with advanced ventilation and filtration systems have become more effective in protecting against exposure to PM of outdoor origin, humans and their activities have emerged as one of the most prominent contributors to the particle burden of the indoor atmosphere [6–10]. Episodic indoor emissions of airborne particles can be associated with exogenous sources related to human activities, including smoking and vaping [11,12], common household activities such as cooking [13–15], candle/incense burning [16,17], vacuuming [18,19], making a bed [20,21], and other general activities that induce the resuspension of indoor dust from flooring and furniture surfaces [22–28]. Particles can also originate from the human body envelope through direct shedding from skin and clothing [29,30], and aerosol release from respiratory activities, such as breathing, talking, and coughing [31–33]. Such emissions from the human envelope can be referred to as endogenous human emissions and have been found to be highly relevant in contributing to personal inhalation exposure to indoor particles, especially biological and abiotic coarse particles larger than 1 μm [34,35].

Establishing a quantitative relationship between localized endogenous and exogenous emission sources and human inhalation intake is a crucial step to assess the relative contribution of emission sources to personal exposure to airborne particles in indoor environments [36]. A direct approach suggested by Lai et al. [37] consists of using a

* Corresponding author.
E-mail address: dusan.licina@epfl.ch (D. Licina).

https://doi.org/10.1016/j.buildenv.2023.110763
Received 5 July 2023; Received in revised form 19 August 2023; Accepted 21 August 2023
Available online 22 August 2023

dimensionless metric referred to as the inhalation transfer factor or the inhalation intake fraction (iF). The inhalation intake fraction is defined as the ratio of the inhaled mass of a pollutant to the total mass ascribed to its given source. iF can be calculated for particles and gases, such as volatile organic compounds [38], and can be determined through both laboratory and field measurements. The inhalation intake fraction is a useful metric that describes the emission-to-inhalation relationship and allows for comparisons among sources with respect to their exposure potential. In addition to age- and activity-specific inhalation rates, iF is dependent on particle transport processes, such as deposition, coagulation, filtration, and ventilation [36], the first three of which vary strongly with particle size. Establishing a database of size-resolved inhalation intake fractions for a diverse array of indoor particle sources and airflow distributions is needed to support exposure and epidemiology studies on the human health implications of indoor-generated particles.

Prior exposure studies have used mathematical models and numerical simulations to estimate the inhalation intake fraction associated with indoor sources, such as tobacco smoking or cooking [15,36]. A common approach among these studies is an assumption of a uniformly mixed indoor atmosphere. In reality, inhalation exposure to indoor air pollutants is often not well characterized using the assumption of perfectly mixed indoor air and uniformly distributed indoor particle concentrations [39,40]. Additional factors that influence evaluation of short-term inhalation exposures from localized indoor PM sources include airflow patterns around the human body [41,42] and the proximity of indoor particle sources to the breathing zone [43,44]. Due to the nature of many household activities, people are often located near emission sources (from a few cm to m) for the duration of the activity, such cooking on a stovetop, cleaning or disinfecting an indoor surface, or physically disturbing settled particle deposits on clothing, flooring, and furniture. Licina et al. [45] found that a well-mixed representation could underestimate the total inhalation intake of coarse particles deliberately released near the body by up to 1.4–1.9-fold. Wu et al. [27] demonstrated that airborne concentrations of resuspended particles in the infant breathing zone can be greater than those in the bulk indoor air by 6 to >10-fold. The ratio of the breathing zone to bulk indoor air concentration was found to increase with particle size from 3 to 11 μm, demonstrating that the high gravitational settling velocities of coarse particles can lead to non-uniformly distributed particle concentrations in indoor microenvironments. The inherent short-duration of episodic indoor particle sources also prevents establishment of uniform particle concentrations throughout an indoor space. In order to better understand the relevance of various particle-phase emission sources associated with human occupancy for indoor exposures, further empirical evidence linking size-resolved inhalation intake fractions with particle emission sources is needed.

An important aspect in characterizing human inhalation exposure in indoor spaces is cross-contamination between occupants, i.e., transmission of particles from one occupant to another. A large body of literature shows that viral aerosol transmission between humans can facilitate the spread of infectious diseases in residential and commercial buildings [46–48]. An empirical study by Licina et al. [30] and a computational fluid dynamics (CFD) modeling study by Al Assaad et al. [49] suggest that the cross-contamination effect can be detected between occupants, but the effect is relatively small in terms of total exposures. However, this effect could be more pronounced with vigorous activities or close distances between occupants.

The aim of this empirical case study is to explore the contribution of human occupancy — through both exogenous and endogenous emissions — to personal inhalation exposures and inhalation intake fractions of fine and coarse particulate matter. Using simultaneous measurements in the occupant's breathing zone and room-average particle concentrations throughout the bulk indoor air, we investigate the variation of the inhalation intake as a function of typical human activities indoors.

2. Materials and methods

2.1. Experimental site

The experiments were conducted in a climatic chamber at the École Polytechnique Fédérale de Lausanne (EPFL) (Switzerland) with a floor area of approximately 25 m^2 and a volume of 60 m^3. The chamber walls are made of painted stainless steel. The ceiling is made of stainless steel panels covered with aluminum foil whereas the floor is made of vinyl. The total internal heat loads were low, consisting of two occupants (200 W), measurement equipment (120 W), and lighting (30 W). The chamber had a dedicated Heating, Ventilation and Air-Conditioning (HVAC) system, which allowed full control of ventilation flow rates, air temperature, and relative humidity (RH). In addition, the chamber had an airtight envelope and conditioned air was supplied and exhausted through two air diffusers located on the ceiling. A 3-stage filtration system (F7 + F9 + high efficiency particulate air (HEPA)) in the supply air duct eliminated nearly all airborne particles from outdoors. This ensured that the measured aerosol signals were exclusively attributed to the presence and activities of the occupant in the chamber. The floor of the chamber is covered with hard vinyl tiles, which is suitable for minimizing particle resuspension [50].

Throughout the experiments, the air temperature was kept at 24 ± 1 °C and RH in the comfortable range of 50 ± 5%. The air exchange rate was maintained constant at 0.7 1/h, common to naturally ventilated family dwellings, throughout all experiments [51]. The air exchange rate was evaluated using the CO_2 tracer gas concentration decay method [52].

2.2. Experimental design and aerosol instrumentation

Table 1 summarizes the experiments designed to investigate the

Table 1
Detailed description of the experiments.

Occupant activity	Scenario/Variable	Clothing condition	Time intervals (min) and activity description
Sitting with moderate movement	Clothing coverage area	Long clean (reference) Short clean	(0–5), (10–15), (20–25): working on computer; (5–10), (15–20), (25–30): stretching head, hands, and legs
	Cleanliness of clothing	Long worn	
Walking	Walking on a clean floor Walking on a used residential carpet	Long clean	(0–30): walking between four marked points at a constant pace (80 steps/min)
Cooking	Breakfast	Long clean	(0–25): French toast fried with butter on electric stove; (25–30): mixed eggs with cheese fried on electric stove
	Lunch		(0–20): boiling pasta on electric stove; (10–30): making a Bolognaise sauce on electric stove
Vacuuming	Vacuuming floor Vacuuming carpet	Long clean	(0–30): vacuuming a floor area corresponding to a single carpet area (0–30): vacuuming a single carpet

inhalation intake fraction of airborne particles associated with human endogenous and exogenous emission sources. A healthy non-smoking male volunteer (Age: 29; height: 174 cm, weight: 83 kg) performed the different scripted experimental scenarios. The volunteer showered the night preceding each experimental day and did not use any skin lotions or moisturizers. Four activity types were included in the experimental design (Table 1): sitting with moderate movement, walking, vacuuming, and cooking. Each activity covered two distinct scenarios. Each experiment was performed for 30 min followed by a 1 h unoccupied period to monitor the decay in particle concentrations. Prior to the experiments, except those including the use of carpets, the floor was thoroughly cleaned with water to minimize particle resuspension.

During the seated activity (Table 1), the influence of clothing coverage area and cleanliness (clean vs. worn) were explored. However, the role of clothing material properties (e.g. thread count, surface roughness) on particle intake fractions was not evaluated in this study. The corresponding chamber configuration is presented in Fig. S1. The long clothing consisted of a long-sleeve t-shirt (100% cotton), trousers, and calf socks (60% cotton, 40% polyester). The short clothing scenario corresponded to short-sleeve t-shirt (100% cotton), shorts, and ankle socks (60% cotton, 40% polyester). Clothing was laundered, tumble-dried, and then exposed for 12 h to indoor residential air. The long clothing ensemble was used as the base clothing condition for the rest of the activities.

The walking activity consisted of two scenarios: the volunteer walking on a clean bare floor with minimum particle resuspension and walking on used un-washed residential carpets. Two used identical carpets (each 170 × 240 cm) located in the same apartment and exposed to the same residential air were utilized in the study. The pile of the carpets is made of 100% polypropylene and the backing from synthetic latex. The carpets were joined to obtain a walking area of 240 × 340 cm^2. Four walking points were marked on the floor and on the carpets on each of the four far corners as illustrated in Fig. 1. The floor walking area was the same as the joined carpets area. The participant walked between the four points at a pace of 80 steps/min regulated by means of a metronome.

For the cooking activity, two experimental runs were conducted using an electric stove during preparation of breakfast and lunch. Making breakfast included making French toast and a cheese omelet, while preparing lunch included boiling pasta and preparing a Bolognaise sauce. The pan used for cooking was made of stainless steel, and there was no exhaust hood present. A detailed description of the scripts of different experimental scenarios is summarized in Table 1. In order to probe the possible effect of cross-contamination between occupants, a breathing thermal manikin was installed in the chamber to mimic the presence of a passive second occupant. The manikin inhalation rate was set to 0.5 m^3/h. During the sitting scenarios, the manikin was placed 2 m away from the occupant. The climate chamber configuration corresponding to cooking activity scenario is shown in Fig. S2.

The vacuuming activity included two scenarios: vacuuming a clean floor and vacuuming used un-washed residential carpets using a dry vacuum cleaner (Model INTERTRONIC Cyclone Cleaner). Vacuuming was performed on the same carpets as used in the walking scenario. To be able to replicate the vacuuming scenarios at different flooring surfaces (bare floor versus carpet), one single carpet and a bare floor area corresponding to dimensions of the carpet were vacuumed in the experimental runs. For the walking, cooking, and vacuuming activities, particle release from the clothing of the volunteer is expected to

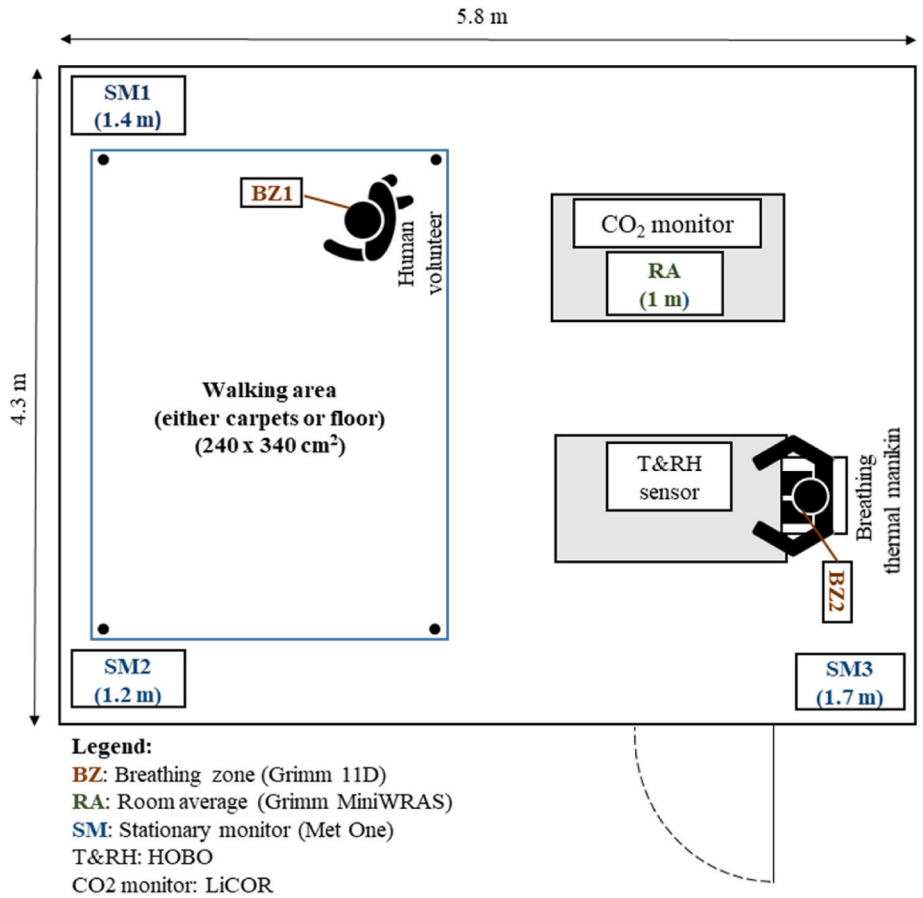

Fig. 1. Climate chamber configuration and particle sampling locations corresponding to the walking scenarios (BZ1 and BZ2: Breathing zone monitors placed within 15 cm from the volunteer's and manikin's mouths, respectively; RA: Room average monitor placed at 1 m above the floor; SM1, SM2 and SM3: Stationary monitors at three heights above the floor: 1.4, 1.2 and 1.7 m, respectively).

influence the measured particle concentrations and size distributions in the breathing zone. However, we expect the influence to be small as the volunteer wore clean clothing during these experiments.

An aerosol spectrometer (Model MiniWRAS 1371, GRIMM Aerosol Technik GmbH; >97% accuracy for the optical measuring range >0.253 μm) was placed in the middle of the chamber to measure room-average particle number concentrations and size distributions. The MiniWRAS measures particles from 0.01 to 35.15 μm across 40 size fractions at a time-resolution of 1 min. Particle measurements in the breathing zone (BZ1) of the occupant were performed using a portable aerosol spectrometer (Model 11D, GRIMM Aerosol Technik GmbH; >95% accuracy for single particle counting). The Model 11D detects particles from 0.253 to 35.15 μm across 31 size fractions at a time-resolution of 1 min. A second aerosol spectrometer (Model MiniWRAS 1371) was installed in the breathing zone of the breathing thermal manikin (BZ2). Three stationary Optical Particle Counters (OPCs) (Model Met One HHPC 6+, Beckman Coulter Life Sciences; manufacturer-specified accuracy ± 10%; counting efficiency: 50% at 0.3 μm and 100% for particles >0.45 μm (per ISO 21501)) were installed at three peripheral locations of the chamber at different heights (1.2 m, 1.4 m, 1.7 m) to assess the spatial uniformity in the emitted particle concentrations within the chamber (Fig. 1). The OPCs measure particles from 0.3 to >10 μm across 6 size fractions at a time-resolution of 1 min. As particles from 0.253/0.3 to >10 μm were optically detected by the aerosol instruments (MiniWRAS, Model 11D, Met One HHPC 6+), the measured particle size can be considered as an optical diameter, and thus, is sensitive to the optical properties (e.g. refractive index) of the measured indoor particles [53].

CO_2 concentrations were continuously monitored during the experiments using a calibrated CO_2 analyzer (Model 820, LI-COR Biosciences). The height of the sample inlet to the CO_2 analyzer was located at 1 m. Both air temperature and RH were continuously monitored during the experiments using a data logger (Model MX1102, HOBO).

2.3. Data analysis and interpretation

Particle emission rates (E) were calculated based on a well-mixed indoor environment assumption. Equation (1) is used to calculate emission rates and is based on the mass balance equation assuming no penetration of particles from outdoors, and ventilation and deposition as the only loss processes for indoor-generated particles.

$$\overline{E_i(T)} = V\left[\frac{(dN_i(T) - dN_i(0))}{T} + (\lambda + \beta_i)\overline{N_i(T)}\right] \quad (1)$$

$E_i(T)$ is time-averaged and size-resolved emission rate per occupant (particles/h) in the size channel i; V is the volume of the chamber (m^3); $N_i(t)$ is the time- and size-resolved indoor particle concentration (particles/m^3) in the size channel i; λ is the air exchange rate of the chamber (1/h); and β_i is the size-resolved particle deposition loss-rate coefficient (1/h) for the size channel i. The overbar represents an average time from 0 to T. The size-resolved particle deposition loss-rate coefficients (β_i) were estimated for each scenario based on the decay of the particle number concentration after the occupant leaves the chamber [54] (Table S1).

The size-resolved inhalation intake fraction was calculated as the ratio of the inhaled particle mass, M_{in}, to the emitted particle mass from the source, M_{rel}, as presented in equation (2):

$$iF_i = \frac{M_{in}}{M_{rel}} = \frac{Q_b \times C_{i,bz}(T)}{E_i(T)} \quad (2)$$

$C_{i,bz}(T)$ is the time-averaged particle mass concentration in the breathing zone (μg/m^3) in the size channel i; $E_i(T)$ is the particle mass emission rate of the source (μg/h) in the size channel i; and Q_b is the inhalation rate (m^3/h). For the seated and cooking scenarios, the inhalation intake fractions were calculated using the recommended inhalation rate for an adult during a light intensity activity from the U.S. EPA Exposure Factors Handbook (Q_b = 0.7 m^3/h) [55]. For the walking and vacuuming scenarios, the Q_b for an adult during a moderate intensity activity (Q_b = 1.5 m^3/h) was used. Size-resolved particle mass concentrations were estimated based on the measured size-resolved particle number concentrations. The mass-weighted size distribution was assumed constant within each size bin. Size-integrated particle mass concentrations (PM_{10}, $PM_{2.5}$) were calculated considering particles larger than 0.3 μm in optical diameter (PM_{10}: 0.3–10 μm, $PM_{2.5}$: 0.3–2.5 μm). Thus, the reported PM_{10} and $PM_{2.5}$ mass concentrations are underestimates of the true values, which account for the mass sub-0.3 μm particles. Particles were assumed spherical (dynamic shape factor (χ) of χ = 1) with a material density equal to 1 g/cm^3 constant across all size bins from 0.3 to 10 μm. Given the range of particle material densities commonly encountered indoors, this calculation method represents a lower-bound estimate of particle mass concentrations [21,56,57].

2.4. Quality assurance

Experiments were randomized and each experiment was replicated at least once, aside for the cooking scenarios that were not replicated. Data collected with the freshly calibrated OPCs were corrected using adjustment factors from side-by-side measurements with all aerosol instruments (Table S2); the adjustment factors for the Met One HHPC 6+ ranged from 0.87 to 1.16 for particles between 0.3 and 10 μm. As a reference in this analysis, we used the newly purchased and calibrated aerosol spectrometer (Grimm 11D). Localized elevations in RH during the cooking experiments may have influenced the output from the OPCs. OPC performance has been shown to degrade for RH > 75% [58]. However, given the tightly controlled RH in the chamber (50 ± 5%) and indoor air mixing conditions, it is unlikely such high RH values were reached in the breathing zone during the experiments.

3. Results and discussion

3.1. Human activities and spatiotemporal variations in coarse particle concentrations

Fig. 2 shows the time-resolved room-average (RA) and breathing zone size-integrated PM_{10} mass concentrations for the occupant (BZ1) and the breathing thermal manikin (BZ2) during the seated, walking, cooking, and vacuuming activities. In three out of four scenarios, the average PM_{10} breathing zone levels of the occupant were higher than the room-average concentrations. During the sitting activities (Fig. 2a), there was a substantial increase in PM_{10} concentrations near the occupant during the stretching periods as compared to the low-activity computer work periods. We note that the excess of particles near the breathing zone relative to the room-average concentrations; also referred to as the personal cloud effect [30,59]; averaged 1.7 μg/m^3 during the 30-min computer activity and 3.4 μg/m^3 during the stretching activity. During this particular scenario, particles detached from the skin and clothing due to occupant movement. Such emissions, in conjunction with low air mixing conditions and the efficient transport by the thermal buoyancy-driven flow of the occupant, caused elevated exposures beyond the room-average levels as similarly found in other studies [30,41,60].

As the walking person (Fig. 2b) mixed the room air well, the personal cloud effect was very low (0.3 μg/m^3) compared to the other activities. The spatial uniformity level assessed using the three stationary OPC monitors (SM1, SM2, and SM3) agreed well with these results. The calculated coefficients of variation for the PM_{10} mass concentrations for the sitting and walking activities were 34% (39% during computer work; 29% during stretching) and 16%, respectively. PM_{10} mass concentrations in BZ1 were generally consistent between the seated stretching (4–6 μg/m^3) and walking (4–8 μg/m^3) activities. However, the composition of the inhaled coarse particles is expected to vary between the two activities, with the former likely associated with clothing fabric fibers,

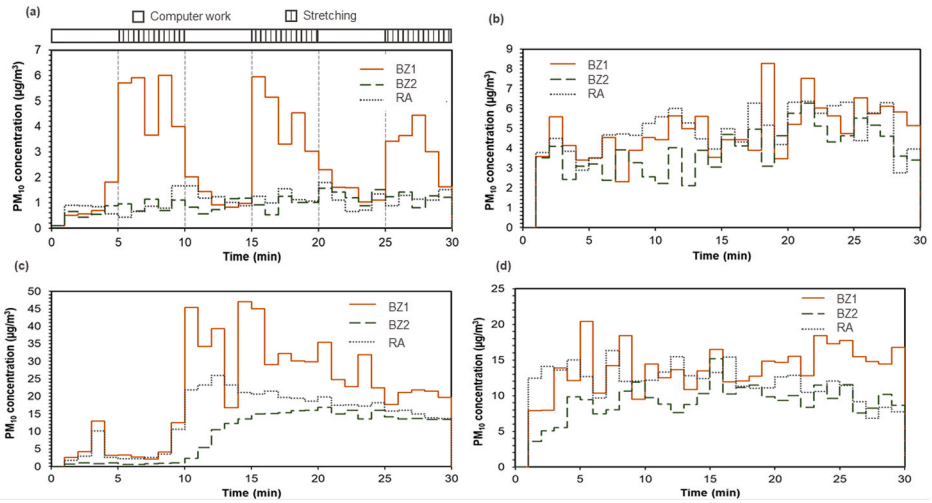

Fig. 2. Time-series with 1-min time-resolution of the PM_{10} mass concentrations for the breathing zone of the occupant (BZ1), the breathing thermal manikin (BZ2), and the room-average (RA) for: (a) seated activity; (b) walking at 80 steps/min on a residential carpet; (c) cooking lunch; and (d) vacuuming a residential carpet.

squames and their fragments, and skin-associated bacteria and yeasts, and the latter likely associated with a larger diversity of deposited biological and abiotic material specific to the residence from which the carpet was located. The observed PM_{10} mass concentrations during sitting and walking would likely scale with the surface loading of particles on clothing and carpet, respectively.

The first 10 min of cooking lunch (pasta boiling) (Fig. 2c) were characterized by relatively low PM_{10} mass concentrations. As expected, the particle concentrations started increasing as the occupant started making the sauce, as similarly found by Buonanno et al. [61]. PM_{10} mass concentrations in the volunteer's breathing zone fluctuated between about 15 and 45 μg/m^3 during much of the cooking activity, the highest levels observed among the four scripted events in the climate chamber. We note that during the sauce making period, the personal cloud effect was discernible, averaging at 10 μg/m^3, and persisting for much of the event. This is due in part to the nature of cooking in modern households, where the breathing zone of a standing occupant is positioned above the stove and cooking apparatus (pot or pan), coincident with the buoyant aerosol-laden frying plume. Preparing the breakfast resulted in similar personal cloud magnitude as cooking the lunch, which was relatively stable throughout the experiment (mean = 12.4 μg/m^3).

Fig. 2d represents the time-series of the vacuuming activity of a residential carpet. Although there was a similarity with the walking scenario, the personal cloud effect was more pronounced (2.2 μg/m^3) due to lower mixing of the room air. A lower personal cloud magnitude was recorded during vacuuming of the floor (1.2 μg/m^3). During vacuuming of the carpet, the measured PM_{10} mass concentrations in BZ1 (10–20 μg/m^3) exceeded that of walking on the same residential carpet, suggesting that the mechanical agitation of carpet fibers, and dust deposits along those fibers, by the vacuum cleaner can enhance particle detachment and resuspension beyond that achieved via footfalls [24]. The range in PM_{10} mass concentrations are consistent with those reported by Corsi et al. [18] (mean of 17 μg/m^3). PM_{10} loadings in the breathing zone are expected to increase for shorter breathing zone heights, such as for infants and children [62–65], as demonstrated in prior measurements and simulations of the vertical gradient in resuspended particle concentrations.

The particle concentrations measured in the breathing zone of the breathing thermal manikin (BZ2) placed 2 m from the occupant during the seated scenario were generally comparable to the room-average concentrations. The room-average concentration and the breathing zone concentration for the breathing thermal manikin were 0.9 μg/m^3 and 1 μg/m^3, respectively. In cases such as walking, cooking, and vacuuming, the concentrations were even lower than the room-average levels due the large distance between the occupant and the breathing thermal manikin (>3 m). However, it is expected that if the breathing thermal manikin was positioned closer to the emission source, PM_{10} mass concentrations in BZ2 would increase.

3.2. Empirical inhalation intake factions for indoor-generated particles

Fig. 3a shows the size-resolved inhalation intake fractions of particles associated with the four investigated indoor activities. The four activities exhibited distinct size-resolved intake fraction profiles between 0.3 and 10 μm. More localized activities, such as cooking or sitting with moderate movement, exhibited a similar uni-modal distribution in the size-resolved intake fraction curve, with a peak at the size range of 1–3 μm. This mode is associated with the dominant size range for human-associated bacteria [66], which might be particularly important when considering shedding from skin or resuspension from clothing, as reported by previous studies [34,67,68]. Seated and cooking activities were also associated with the highest intake fractions of the four activities due to the proximity of the exposed person to the emission source and the enhanced transport of particles by means of the buoyant thermal plume [41,60].

For activities with more human motion (walking and vacuuming), the intake fraction was consistently lower, particularly for super-micron particles between 1 and 10 μm. This is attributed to an absence of the buoyant thermal plume around a human body due to constant movements (Licina et al. [45]), and enhanced gravitational settling of resuspended particles to indoor surfaces at elevated air speeds (Thatcher et al. [54]). However, in contrast to sitting and cooking, the inhalation intake fractions for walking on a clean floor and vacuuming a residential carpet increased with decreasing particle size between 0.3 and 10 μm, with the maximum intake fractions observed in the smallest size fraction of the optical-based aerosol instrumentation (0.3–0.5 μm). This unique size-dependent trend is consistent with the size-resolved intake fractions reported by Boor et al. [21] and Spilak et al. [26] for human movement-induced mattress dust resuspension and by Wu et al. [27] for infant crawling-induced floor dust resuspension. A number of factors can explain the observed size-dependency in the intake fractions, including the significant abundance of sub-1 μm particles in floor dust and the increase in the size-dependent particle deposition loss-rate coefficient with particle size between 0.3 and 10 μm (Table S1). The mean

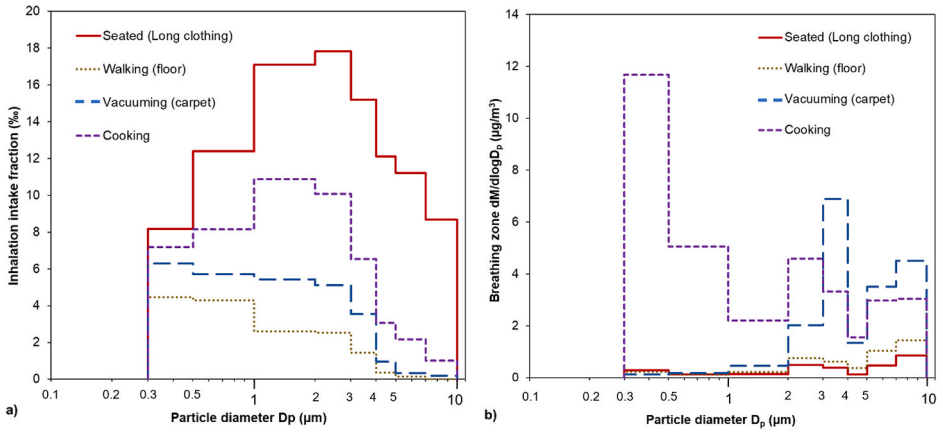

Fig. 3. (a) Size-resolved average inhalation intake fractions of particles during four indoor scenarios: seated with long clean clothing (reference scenario), walking on a clean floor at 80 steps/min, vacuuming a residential carpet, and cooking breakfast (French toast and omelet), (b) Size-resolved breathing zone particle mass concentrations associated with the same scenarios.

deposition rate for 0.3–0.5 μm particles was 0.13 1/h for walking and vacuuming, much less than that observed for 5–10 μm particles (4.82–5.23 1/h). Thus, a resuspended particle 0.5 μm in size will have a greater likelihood of being inhaled, rather than be removed via gravitational settling to horizontal upward-facing indoor surfaces, compared to a 5 μm particle.

The breathing zone size-resolved particle mass concentrations (dM/dlogD_p) corresponding to the four activities are presented in Fig. 3b. Results of the comparison in the breathing zone PM_{10} mass concentrations among the three clothing experiments (Table 1) for the seated activity is summarized in Fig. S3. The particle mass size distributions for cooking exhibited a bi-modal shape and were dominated by sub-micron particles (0.3–1 μm). Conversely, those for vacuuming a residential carpet were dominated by coarse mode particles, with the highest mass concentrations observed in the 3–4 μm size bin. Sitting and walking exhibited bi-modal particle mass size distributions, with modes of 2–4 μm and 5–10 μm. The 2–4 μm mode has been documented in prior observations of coarse mode particle emissions from occupants, including skin shedding and clothing and floor dust resuspension [6,29,30,34,45,65,67–70]. This mode is important from a personal exposure perspective as it coincides with the local maxima in the size-resolved particle deposition fraction curve for the pulmonary region [65].

Interestingly, the modes measured for the size-resolved particle mass concentrations were not consistent with those observed in the size-resolved inhalation intake fraction profiles. This suggests the complex nature of the source-receptor relationship, which accounts for the size-dependency of the emitted and inhaled aerosol population and associated transport processes of relevance to indoor environments, along with breathing zone proximity effects and indoor air mixing conditions. Although size-resolved particle mass concentrations in the volunteer's breathing zone were greater for the exogenous sources, emissions from clothing and skin during the seated scenarios were associated with the highest total inhalation intake fraction (13‰). It should also be noted that even though variation in cooking (breakfast vs. lunch) and vacuuming activities (floor vs. carpet) resulted in distinct breathing zone concentrations, relative differences in inhalation intake fractions were small.

3.3. Inhalation intake fractions in a perfectly mixed indoor environment

In order to compare our empirical results to those estimated using a perfectly mixed indoor environment, we used a modelling approach described by Nazaroff [36] for non-reactive and non-sorbing air pollutants. The calculation considers both removal of particles by ventilation and deposition and considers that the air is instantly perfectly mixed in an indoor space:

$$iF_i = \frac{Q_b}{Q+\beta_i V}\left[1-\frac{V}{QT}\left(1-exp\left(-\frac{(Q+\beta_i V)T}{V}\right)\right)\right] \quad (3)$$

In equation (3), Q_b is the inhalation rate (m^3/h); Q is the chamber ventilation flow rate (m^3/h); β_i is the particle deposition loss-rate coefficient (1/h) for the size channel i, V is the volume of the chamber (m^3); and T is the time until the end of the experiment (h). As for the calculation of the empirical intake fraction, we used the recommended inhalation rate for a light intensity activity for the seated and cooking scenarios and the Q_b value for moderate intensity activities for the walking and vacuuming activities.

Fig. 4 shows that regardless of the emission source, modelled inhalation intake fraction values remained nearly the same (average intake fraction = 4‰) when the indoor air is assumed to be instantly perfectly mixed. Relative to a perfectly mixed environment, the empirical intake fractions were generally greater for most of the scenarios. The greater the extent of the personal cloud effect (Fig. 2), the higher was the discrepancy between empirical and idealized intake fractions. Although activities such as cooking or vacuuming a carpet were associated with stronger PM_{10} emission sources (ER = 1209–2134 μg/h), the inhalation intake fractions were not higher than the sitting activity, which had the lowest emission rate (ER = 111 μg/h). For the seated and cooking activities, the empirical inhalation intake fractions were underestimated by 3.2-fold and 2.3-fold, respectively, compared to the well mixed indoor air assumption. For the walking activity, since the walking occupant mixes the room air efficiently, the predicted intake fraction using the perfectly mixed environment assumption was similar to the empirically calculated value. The partially-localized movement of the occupant in one half of the chamber during the vacuuming activity contributed to relatively better mixing than the seated activity. The empirical intake fraction (5.7‰) was only 1.4 times higher than the well mixed value in this case.

The results presented in Fig. 4 demonstrate the importance of directly measuring particle concentrations in the breathing zone and using such measurements to derive accurate estimations of particle inhalation intake fractions and other exposure metrics, such as the respiratory tract deposited dose rate. This is especially true when the breathing zone concentration deviates significantly from the room-average concentration measured in the bulk indoor air (Fig. 2). However, real-time breathing zone measurements of particles with conventional aerosol instrumentation is challenging in field conditions due to the size and power requirements of the equipment. Recently developed low-cost, battery-powered OPCs can track coarse mode particle levels in

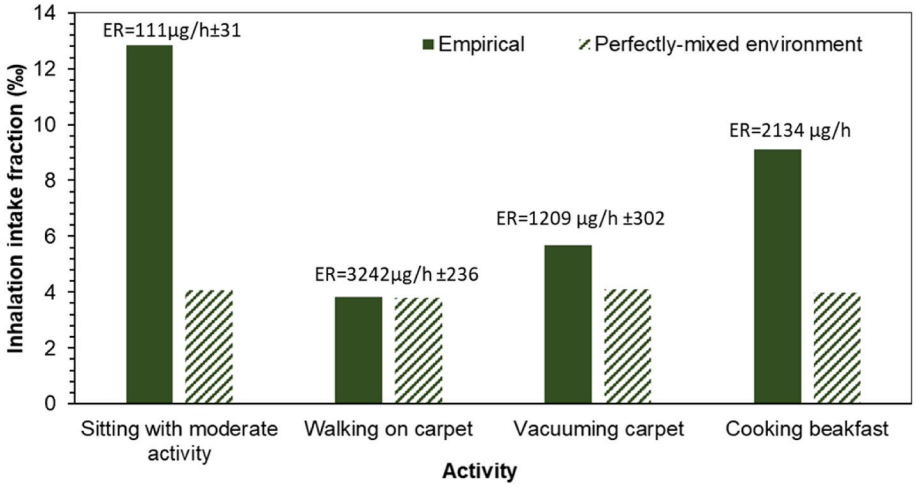

Fig. 4. Empirically-derived inhalation intake fractions for particles (0.3–10 µm) compared to intake fractions estimated assuming a perfectly mixed indoor environment. All presented activities refer to clean clothing scenario.

the occupant's breathing zone, thereby providing a basis for improved estimates of inhalation intake fractions in real-world scenarios. Furthermore, future studies can pair multi-location OPC measurements with computational fluid dynamics (CFD) simulations [71] to better characterize spatial variations in personal exposures to particles under different ventilation conditions and to quantify the uncertainty in using the perfectly mixed environment assumption to evaluate particle intake fractions.

3.4. Variations in outdoor and indoor inhalation intake fractions for particles

Fig. 5 summarizes the range in empirical inhalation intake fractions determined in this study for four human activities, along with those previously reported for a variety of outdoor and indoor emission sources. This study contributes to the limited database of empirically-based intake fractions derived for personal aerosol exposure measurements in the breathing zone. Intake fractions are expressed in Fig. 5 as the number of particles inhaled per million emitted from a source (or ppm). Thus, an iF of 1 ppm indicates that for every million particles emitted, one particle is inhaled, or for every kg emitted, one mg is inhaled. Outdoor inhalation intake fractions are generally in the range of 10°-10^{2} ppm, whereas indoor intake fractions range from 10^{3} to 10^{5} ppm. The three orders of magnitude difference between outdoor and indoor particle intake fractions has been referred to as the rule of 1000 [37]. Thus, a typical particle release indoors due to particle resuspension from clothing or flooring, as documented in this chamber study, is about 1000 times more effective in producing a particle exposure than an outdoor source, such as ground-level line sources (e.g. vehicle exhaust). This is due in part to the proximity effect inherent to many indoor particle sources, whereby the breathing zone is often a few cm to m from actively emitting indoor sources that are present in poorly diluted indoor atmospheres.

As demonstrated in Fig. 5, endogenous particle emission sources associated with skin and clothing are associated with some of the largest reported inhalation intake fractions (10^{5} ppm) among all outdoor and indoor sources. Such sources are typically not considered in conventional air pollution risk assessments, yet they are highly efficient at

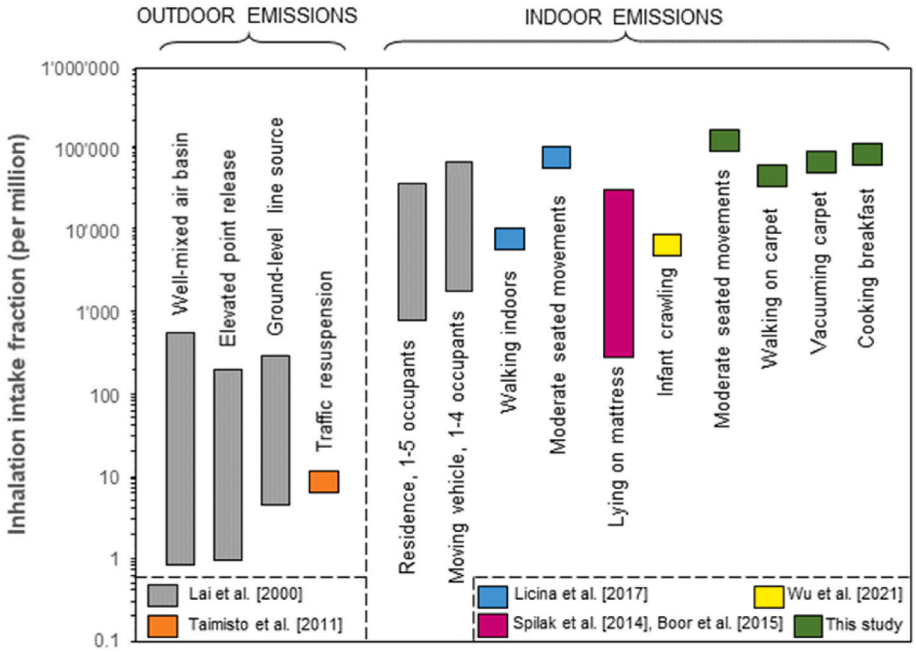

Fig. 5. Summary of ranges in inhalation intake fractions (per million, ppm) reported for (left) outdoor emission sources, including a well-mixed air basin, elevated point release, ground-level line source (Lai et al. [37]), and traffic-induced particle resuspension (Taimisto et al. [72]) and (right) indoor emission sources, including: residence, 1–5 occupants, interior of a moving vehicle, 1–4 occupants (Lai et al. [37]), walking indoors, moderate seated movements (Licina et al. [45]), mattress dust resuspension (1–5 µm and 5–20 µm size fractions) (Spilak et al. [26]; Boor et al. [21]), infant crawling-induced floor dust resuspension (Wu et al. [27]), and the four scripted activities evaluated in this study: moderate seated movements, walking on carpet, vacuuming carpet, and cooking breakfast. Modelling data are shown in gray color. (For interpretation of the references to color in this figure legend, the reader is referred to the Web version of this article.)

producing an exposure relative to the magnitude of their emissions. Intake fractions for indoor particle resuspension on various surfaces due to different human movements can range from $<10^3$ ppm on the lower end to about 4×10^4 ppm on the upper end (Fig. 5). As the inhalation intake fraction scales with the inhalation rate, intake fractions for adult walking-induced dust resuspension are greater than those for infant crawling-induced dust resuspension. The particle intake fractions presented in Fig. 5 will vary with age- and activity-specific inhalation rates and indoor air mixing conditions specific to a room or building. Such factors need to be considered in applying intake fractions when evaluating source-oriented health risks. The indoor inhalation intake fractions for particles presented in Fig. 5 can be combined with data on activity pattern surveys [4] and source-specific particle number and mass emission rates [73] to derive estimates of daily personal exposures as total number or mass of airborne particles inhaled per day (Equation (2)). Such an analysis can provide a basis to understand how different particle sources contribute to personal exposures in residential indoor environments.

3.5. Study limitations

There are several limitations associated with the present investigation. First, only four common human activities were considered under the airflow conditions specific to the climate chamber. Future controlled chamber studies are therefore needed to develop a database of size-resolved inhalation intake fractions for particles released from different indoor sources under variable indoor air mixing conditions. Second, the inhalation intake fraction analysis only focused on fine and coarse particles from 0.3 to 10 μm and may not represent intake fractions for sub-100 nm ultrafine particles due to differences in emission, deposition, and transformation processes that can affect the source-receptor relationship. Third, most of the scenarios were only conducted twice by one volunteer and thus, may not provide an accurate assessment of person-to-person variability (e.g. due to height, clothing type) in inhalation intake fractions. Fourth, the dust loading on the carpets was not determined in this study, thus, care should be taken in extrapolating the intake fraction results to carpets with variable dust loadings. However, human-induced particle resuspension studies have found that resuspended particle concentrations do not necessarily correlate well with dust loadings due to the complexity of the resuspension process from carpet fibers [27]. Thus, relating inhalation intake fractions to carpet dust loadings may not be trivial.

4. Conclusions

The inhalation intake fraction metric is useful to compare exposures to pollutants released under different scenarios and to conduct preliminary health risk assessments. The present study investigates the variation of the inhalation intake fraction associated with four scripted activities in a controlled climate chamber. Our findings suggest that the assumption of a well-mixed indoor environment could underestimate inhalation exposures to particles by up to 3.2-fold in spaces typically occupied by humans. The results also confirm that the inhalation intake fraction depends primarily on the degree of motion related to the indoor activity and the proximity of the source to the exposed individual, rather than the strength of the source itself. The inhalation intake fraction associated with endogenous human emissions, although often underestimated, was larger than the intake fraction associated with exogenous sources. The analysis showed that emissions from clothing and skin during the seated scenarios were associated with the highest total inhalation intake fractions (13‰), followed by cooking (9‰), vacuuming (5.7‰), and walking (3.9‰). Additional efforts are required to characterize the different endogenous emission mechanisms and their influence on personal inhalation exposure to fine and coarse particles. The results from this empirical study can help improve our understanding on variations in the inhalation intake fraction associated with different common indoor activities and corresponding health risk assessments for indoor particles.

CRediT authorship contribution statement

Dusan Licina: Visualization, Resources, Project administration, Methodology, Investigation, Funding acquisition, Formal analysis, Conceptualization, Writing – original draft. **Brandon E. Boor:** Writing – original draft.

Declaration of competing interest

The authors declare that they have no known competing financial interests or personal relationships that could have appeared to influence the work reported in this paper.

Data availability

Data will be made available on request.

Acknowledgments

This study was funded by the Swiss National Science Foundation (SNSF), Grant number: 205321_192086. Special thanks to Mr. Marouane Merizak for assisting with the project and to Dr. Shen Yang for providing the two residential carpets used in the study.

Appendix A. Supplementary data

Supplementary data to this article can be found online at https://doi.org/10.1016/j.buildenv.2023.110763.

References

[1] A. Peters, D.W. Dockery, J.E. Muller, M.A. Mittleman, Increased particulate air pollution and the triggering of myocardial infarction, Circulation 103 (23) (2001) 2810–2815, https://doi.org/10.1161/01.CIR.103.23.2810.

[2] O. Morakinyo, M. Mokgobu, M. Mukhola, R. Hunter, Health outcomes of exposure to biological and chemical components of inhalable and respirable particulate matter, Int. J. Environ. Res. Publ. Health 13 (6) (2016) 592, https://doi.org/10.3390/ijerph13060592.

[3] O. Raaschou-Nielsen, Z.J. Andersen, R. Beelen, E. Samoli, M. Stafoggia, G. Weinmayr, B. Hoffmann, P. Fischer, M.J. Nieuwenhuijsen, B. Brunekreef, W. W. Xun, K. Katsouyanni, K. Dimakopoulou, J. Sommar, B. Forsberg, L. Modig, A. Oudin, B. Oftedal, P.E. Schwarze, P. Nafstad, U. De Faire, N.L. Pedersen, C.-G. Östenson, L. Fratiglioni, J. Penell, M. Korek, G. Pershagen, K.T. Eriksen, M. Sørensen, A. Tjønneland, T. Ellermann, M. Eeftens, P.H. Peeters, K. Meliefste, M. Wang, B. Bueno-de-Mesquita, T.J. Key, K. de Hoogh, H. Concin, G. Nagel, A. Vilier, S. Grioni, V. Krogh, M.-Y. Tsai, F. Ricceri, C. Sacerdote, C. Galassi, E. Migliore, A. Ranzi, G. Cesaroni, C. Badaloni, F. Forastiere, I. Tamayo, P. Amiano, M. Dorronsoro, A. Trichopoulou, C. Bamia, P. Vineis, G. Hoek, Air pollution and lung cancer incidence in 17 European cohorts: prospective analyses from the European study of cohorts for air pollution effects (ESCAPE), Lancet Oncol. 14 (9) (2013) 813–822, https://doi.org/10.1016/S1470-2045(13)70279-1.

[4] N.E. Klepeis, W.C. Nelson, W.R. Ott, J.P. Robinson, A.M. Tsang, P. Switzer, J. V. Behar, S.C. Hern, W.H. Engelmann, The national human activity pattern survey (NHAPS): a resource for assessing exposure to environmental pollutants, J. Expo. Sci. Environ. Epidemiol. 11 (3) (2001) 231–252, https://doi.org/10.1038/sj.jea.7500165.

[5] J. Zhou, A. Chen, Q. Cao, B. Yang, V.W.-C. Chang, W.W. Nazaroff, Particle exposure during the 2013 haze in Singapore: importance of the built environment, Build. Environ. 93 (2015) 14–23, https://doi.org/10.1016/j.buildenv.2015.04.029.

[6] D. Licina, S. Bhangar, B. Brooks, R. Baker, B. Firek, X. Tang, M.J. Morowitz, J. F. Banfield, W.W. Nazaroff, Concentrations and sources of airborne particles in a neonatal intensive care unit, PLoS One 13 (5) (2016), e0154991, https://doi.org/10.1371/journal.pone.0154991, 11.

[7] A. Avery, M.S. Waring, P.F. DeCarlo, Human occupant contribution to secondary aerosol mass in the indoor environment, Environ. Sci. Process Impacts 21 (2019) 1301–1312, https://doi.org/10.1039/C9EM00097F.

[8] S. Yang, A. Muthalagu, V.G. Serrano, D. Licina, Human personal air pollution clouds in a naturally ventilated office during the COVID-19 pandemic, Build. Environ. 15 (2023), 110280, https://doi.org/10.1016/j.buildenv.2023.110280, 236.

[9] S. Patel, S. Sankhyan, E.K. Boedicker, P.F. DeCarlo, D.K. Farmer, A.H. Goldstein, E. F. Katz, W.W. Nazaroff, Y. Tian, J. Vanhanen, M.E. Vance, Indoor particulate matter during HOMEChem: concentrations, size distributions, and exposures,

Environ. Sci. Technol. 16 (12) (2020) 7107–7116, https://doi.org/10.1021/acs.est.0c00740, 54.
[10] D.K. Farmer, M.E. Vance, J.P.D. Abbatt, A. Abeleira, M.R. Alves, C. Arata, E. Boedicker, S. Bourne, F. Cardoso-Saldaña, R. Corsi, P.F. DeCarlo, A.H. Goldstein, V.H. Grassian, L.H. Ruiz, J.L. Jimenez, T.F. Kahan, E.F. Katz, J.M. Mattila, W. W. Nazaroff, A. Novoselac, R.E. O'Brien, V.W. Or, S. Patel, S. Sankhyan, P. S. Stevens, Y. Tian, M. Wade, C. Wang, S. Zhou, Y. Zhou, Overview of HOMEChem: house observations of microbial and environmental chemistry, Environ. Sci. Process. Impacts 21 (8) (2019) 1280–1300, https://doi.org/10.1039/C9EM00228F.
[11] Z. Ning, C.S. Cheung, J. Fu, M.A. Liu, M.A. Schnell, Experimental study of environmental tobacco smoke particles under actual indoor environment, Sci. Total Environ. 367 (2–3) (2006) 822–830, https://doi.org/10.1016/j.scitotenv.2006.02.017.
[12] K. Slezakova, M.C. Pereira, M.C. Alvim-Ferraz, Influence of tobacco smoke on the elemental composition of indoor particles of different sizes, Atmos. Environ. 43 (3) (2009) 486–493, https://doi.org/10.1016/j.atmosenv.2008.10.017.
[13] T. Hu, B.C. Singer, J.M. Logue, Compilation of Published PM2.5 Emission Rates for Cooking, Candles and Incense for Use in Modeling of Exposures in Residences, LBNL–5890E, 1172959, 2012, 1172959, https://doi.org/10.2172/1172959. LBNL–5890E.
[14] C.A. Alves, E.D. Vicente, M. Evtyugina, A.M.P. Vicente, T.-A. Sainnokhoi, N. Kováts, Cooking activities in a domestic kitchen: chemical and toxicological profiling of emissions, Sci. Total Environ. 772 (2021), 145412, https://doi.org/10.1016/j.scitotenv.2021.145412.
[15] J. Gao, C. Cao, Q. Xiao, B. Xu, X. Zhou, X. Zhang, Determination of dynamic intake fraction of cooking-generated particles in the kitchen, Build. Environ. 65 (2013) 146–153, https://doi.org/10.1016/j.buildenv.2013.04.006.
[16] C. Andersen, Y. Omelekhina, B.B. Rasmussen, M. Nygaard Bennekov, S.N. Skov, M. Køcks, K. Wang, B. Strandberg, F. Mattsson, M. Bilde, M. Glasius, J. Pagels, A. Wierzbicka, Emissions of soot, PAHs, ultrafine particles, NOx, and other health relevant compounds from stressed burning of candles in indoor air, Indoor Air 31 (6) (2021) 2033–2048, https://doi.org/10.1111/ina.12909.
[17] X. Ji, O. Le Bihan, O. Ramalho, C. Mandin, B. D'Anna, L. Martinon, M. Nicolas, D. Bard, J.C. Pairon, Characterization of particles emitted by incense burning in an experimental house, Indoor Air 20 (2) (2010) 147–158, https://doi.org/10.1111/j.1600-0668.2009.00634.x.
[18] R.L. Corsi, J.A. Siegel, C. Chiang, Particle resuspension during the use of vacuum cleaners on residential carpet, J. Occup. Environ. Hyg. 5 (4) (2008) 232–238, https://doi.org/10.1080/15459620801901165.
[19] L.D. Knibbs, C. He, C. Duchaine, L. Morawska, Vacuum cleaner emissions as a source of indoor exposure to airborne particles and bacteria, Environ. Sci. Technol. 46 (1) (2012) 534–542, https://doi.org/10.1021/es202946w.
[20] A.R. Ferro, R.J. Kopperud, L.M. Hildemann, Source strengths for indoor human activities that resuspend particulate matter, Environ. Sci. Technol. 38 (6) (2004) 1759–1764, https://doi.org/10.1021/es0263893.
[21] B.E. Boor, M.P. Spilak, R.L. Corsi, A. Novoselac, Characterizing particle resuspension from mattresses: chamber study, Indoor Air 25 (4) (2015) 441–456, https://doi.org/10.1111/ina.12148.
[22] A.R. Ferro, R.J. Kopperud, L.M. Hildemann, Elevated personal exposure to particulate matter from human activities in a residence, J. Expo. Sci. Environ. Epidemiol. 14 (S1) (2004) S34–S40, https://doi.org/10.1038/sj.jea.7500356.
[23] W.W. Nazaroff, B.C. Singer, Inhalation of hazardous air pollutants from environmental tobacco smoke in US residences, J. Expo. Sci. Environ. Epidemiol. 14 (S1) (2004) S71–S77, https://doi.org/10.1038/sj.jea.7500361.
[24] J. Qian, J. Peccia, A.R. Ferro, Walking-induced particle resuspension in indoor environments, Atmos. Environ. 89 (2014) 464–481, https://doi.org/10.1016/j.atmosenv.2014.02.035.
[25] L.M. Milstone, Epidermal desquamation, J. Dermatol. Sci. 36 (3) (2004) 131–140, https://doi.org/10.1016/j.jdermsci.2004.05.004.
[26] P.M. Spilak, E.B. Boor, A. Novoselac, L.R. Corsi, Impact of bedding arrangements, pillows, and blankets on particle resuspension in the sleep microenvironment, Build. Environ. 81 (2014) 60–68, https://doi.org/10.1016/j.buildenv.2014.06.010.
[27] T. Wu, M. Fu, M. Valkonen, M. Täubel, Y. Xu, E.B. Boor, Particle resuspension dynamics in the infant near-floor microenvironment, Environ. Sci. Technol. 55 (3) (2021) 1864–1875, https://doi.org/10.1021/acs.est.0c06157.
[28] S.Y. Yang, H.H. Zhang, T.C. Hsiao, A.R. Ferro, A.C.K. Lai, Evaluation of human walking-induced resuspension of bacteria on different flooring materials, Build. Environ. 235 (2023), 110218, https://doi.org/10.1016/j.buildenv.2023.110218.
[29] D. Licina, W.W. Nazaroff, Clothing as a transport vector for airborne particles: chamber study, Indoor Air 28 (3) (2018) 404–414, https://doi.org/10.1111/ina.12452.
[30] D. Licina, Y. Tian, W.W. Nazaroff, Emission rates and the personal cloud effect associated with particle release from the perihuman environment, Indoor Air 27 (4) (2017) 791–802, https://doi.org/10.1111/ina.12365.
[31] T. Stockman, S. Zhu, A. Kumar, L. Wang, S. Patel, J. Weaver, M. Spede, D.K. Milton, J. Hertzberg, D. Toohey, M. Vance, J. Srebric, S.L. Miller, Measurements and simulations of aerosol released while singing and playing wind instruments, ACS Environ. Au 1 (1) (2021) 71–84, https://doi.org/10.1021/acsenvironau.1c00007.
[32] M. Alsved, A. Matamis, R. Bohlin, M. Richter, P.E. Bengtsson, C.-J. Fraenkel, P. Medstrand, J. Löndahl, Exhaled respiratory particles during singing and talking, Aerosol Sci. Technol. 54 (11) (2020) 1245–1248, https://doi.org/10.1080/02786826.2020.1812502.
[33] S. Asadi, A.S. Wexler, C.D. Cappa, S. Barreda, N.M. Bouvier, W.D. Ristenpart, Aerosol emission and superemission during human speech increase with voice loudness, Sci. Rep. 9 (1) (2019) 2348, https://doi.org/10.1038/s41598-019-38808-z, 20.
[34] S. Yang, G. Bekö, P. Wargocki, J. Williams, D. Licina, Human emissions of size-resolved fluorescent aerosol particles: influence of personal and environmental factors, Environ. Sci. Technol. 55 (1) (2021) 509–518, https://doi.org/10.1021/acs.est.0c06304.
[35] V. González Serrano, D. Licina, Longitudinal assessment of personal air pollution clouds in ten home and office environments, Indoor Air 32 (2) (2022), https://doi.org/10.1111/ina.12993.
[36] W.W. Nazaroff, Inhalation intake fraction of pollutants from episodic indoor emissions, Build. Environ. 43 (3) (2008) 269–277, https://doi.org/10.1016/j.buildenv.2006.03.021.
[37] A.C.K. Lai, T.L. Thatcher, W.W. Nazaroff, Inhalation transfer factors for air pollution health risk assessment, J. Air Waste Manag. Assoc. 50 (9) (2000) 1688–1699, https://doi.org/10.1080/10473289.2000.10464196.
[38] J. Jiang, X. Ding, A. Tasoglou, H. Huber, D.A. Shah, N. Jung, E.B. Boor, Real-time measurements of botanical disinfectant emissions, transformations, and multiphase inhalation exposures in buildings, Environ. Sci. Technol. Lett. 8 (7) (2021) 558–566, https://doi.org/10.1021/acs.estlett.1c00390.
[39] J.S. Russo, H. Ezzat Khalifa, CFD assessment of intake fraction in the indoor environment, Build. Environ. 45 (9) (2010) 1968–1975, https://doi.org/10.1016/j.buildenv.2010.01.017.
[40] N.E. Klepeis, Validity of the uniform mixing assumption: determining human exposure to environmental tobacco smoke, Environ. Health Perspect. 107 (1999) 7, https://doi.org/10.1289/ehp.99107s2357.
[41] D. Licina, A. Melikov, J. Pantelic, C. Sekhar, K.W. Tham, Human convection flow in spaces with and without ventilation: personal exposure to floor-released particles and cough-released droplets, Indoor Air 25 (6) (2015) 672–682, https://doi.org/10.1111/ina.12177.
[42] D. Licina, J. Pantelic, A. Melikov, C. Sekhar, K.W. Tham, Experimental investigation of the human convective boundary layer in a quiescent indoor environment, Build. Environ. 75 (2014) 79–91, https://doi.org/10.1016/j.buildenv.2014.01.016.
[43] E. Tielemans, T. Schneider, H. Goede, M. Tischer, N. Warren, H. Kromhout, M. Van Tongeren, J. Van Hemmen, J.W. Cherrie, Conceptual model for assessment of inhalation exposure: defining modifying factors, Ann. Occup. Hyg. 51 (2008) 577–586, https://doi.org/10.1093/annhyg/men059.
[44] S.J. Mcbride, A.R. Ferro, W.R. Ott, P. Switzer, L.M. Hildemann, Investigations of the proximity effect for pollutants in the indoor environment, J. Expo. Sci. Environ. Epidemiol. 9 (6) (1999) 602–621, https://doi.org/10.1038/sj.jea.7500057.
[45] D. Licina, Y. Tian, W.W. Nazaroff, Inhalation intake fraction of particulate matter from localized indoor emissions, Build. Environ. 123 (2017) 14–22, https://doi.org/10.1016/j.buildenv.2017.06.037.
[46] J.S. Kutter, M.I. Spronken, P.L. Fraaij, R.A. Fouchier, S. Herfst, Transmission routes of respiratory viruses among humans, Curr. Opin. Virol. 28 (2018) 142–151, https://doi.org/10.1016/j.coviro.2018.01.001.
[47] S. Herfst, M. Böhringer, B. Karo, P. Lawrence, N.S. Lewis, M.J. Mina, C.J. Russell, J. Steel, R.L. de Swart, C. Menge, Drivers of airborne human-to-human pathogen transmission, Curr. Opin. Virol. 22 (2017) 22–29, https://doi.org/10.1016/j.coviro.2016.11.006.
[48] L. Morawska, J. Cao, Airborne transmission of SARS-CoV-2: the world should face the reality, Environ. Int. 139 (2020), 105730, https://doi.org/10.1016/j.envint.2020.105730.
[49] D. Al Assaad, S. Yang, D. Licina, Particle release and transport from human skin and clothing: a CFD modeling methodology, Indoor Air 31 (2021) 1377–1390, https://doi.org/10.1111/ina.12840.
[50] J. Qian, A.R. Ferro, Resuspension of dust particles in a chamber and associated environmental factors, Aerosol Sci. Technol. 42 (7) (2008) 566–578, https://doi.org/10.1080/02786820802220274.
[51] G. Bekö, T. Lund, F. Nors, J. Toftum, G. Clausen, Ventilation rates in the bedrooms of 500 Danish children, Build. Environ. 45 (10) (2010) 2289–2295, https://doi.org/10.1016/j.buildenv.2010.04.014.
[52] G. Remion, B. Moujalled, M. El Mankibi, Review of tracer gas-based methods for the characterization of natural ventilation performance: comparative analysis of their accuracy, Build. Environ. 160 (2019), 106180, https://doi.org/10.1016/j.buildenv.2019.106180.
[53] S.S. Patra, R. Ramsisaria, R. Du, T. Wu, E.B. Boor, A machine learning field calibration method for improving the performance of low-cost particle sensors, Build. Environ. 190 (2021), 107457, https://doi.org/10.1016/j.buildenv.2020.107457.
[54] T.L. Thatcher, A.C.K. Lai, R. Moreno-Jackson, R.G. Sextro, W.W. Nazaroff, Effects of room furnishings and air speed on particle deposition rates indoors, Atmos. Environ. 36 (11) (2002) 1811–1819, https://doi.org/10.1016/S1352-2310(02)00157-7.
[55] U.S. EPA (Environmental Protection Agency, Exposure Factors Handbook: 2011 Edition, National Center for Environmental Assessment, Washington, DC, 2011. ; EPA/600/R-09/052F. Available from: the National Technical Information Service, Springfield, VA, and online at, http://www.epa.gov/ncea/efh.
[56] M. Pitz, J. Cyrys, E. Karg, A. Wiedensohler, H.-E. Wichmann, J. Heinrich, Variability of apparent particle density of an urban aerosol, Environ. Sci. Technol. 37 (19) (2003) 4336–4342, https://doi.org/10.1021/es034322p.
[57] Z. Wang, W.W. Delp, B.C. Singer, Performance of low-cost indoor air quality monitors for PM2.5 and PM10 from residential sources, Build. Environ. 171 (2020), 106654, https://doi.org/10.1016/j.buildenv.2020.106654.

[58] P. Wang, F. Xu, H. Wang, D.-R. Chen, Effect of relative humidity on the performance of five cost-effective PM sensors, Aerosol Sci. Technol. 55 (8) (2021) 957–974, https://doi.org/10.1080/02786826.2021.1910136.
[59] R. You, W. Cui, C. Chen, B. Zhao, Measuring the short-term emission rates of particles in the "personal cloud" with different clothes and activity intensities in a sealed chamber, Aerosol Air Qual. Res. 13 (3) (2013) 911–921, https://doi.org/10.4209/aaqr.2012.03.0061.
[60] D. Rim, A. Novoselac, Occupational exposure to hazardous airborne pollutants: effects of air mixing and source location, J. Occup. Environ. Hyg. 7 (12) (2010) 683–692, https://doi.org/10.1080/15459624.2010.526894.
[61] G. Buonanno, L. Morawska, L. Stabile, Particle emission factors during cooking activities, Atmos. Environ. 43 (20) (2009) 3235–3242, https://doi.org/10.1016/j.atmosenv.2009.03.044.
[62] P. Khare, L.C. Marr, Simulation of vertical concentration gradient of influenza viruses in dust resuspended by walking, Indoor Air 25 (4) (2015) 428–440, https://doi.org/10.1111/ina.12156.
[63] S.L. Shalat, A.A. Stambler, Z. Wang, G. Mainelis, O.H. Emoekpere, M. Hernandez, P.J. Lioy, K. Black, Development and in-home testing of the pretoddler inhalable particulate environmental robotic (PIPER mk IV) sampler, Environ. Sci. Technol. 1 (7) (2011) 2945–2950, https://doi.org/10.1021/es1033876, 45.
[64] Z. Wang, S.L. Shalat, K. Black, P.J. Lioy, A.A. Stambler, O.H. Emoekpere, M. Hernandez, T. Han, M. Ramagopal, G. Mainelis, Use of a robotic sampling platform to assess young children's exposure to indoor bioaerosols, Indoor Air 22 (2) (2012) 159–169, https://doi.org/10.1111/j.1600-0668.2011.00749.x.
[65] T. Wu, M. Täubel, R. Holopainen, A.K. Viitanen, S. Vainiotalo, T. Tuomi, J. Keskinen, A. Hyvärinen, K. Hämeri, S.E. Saari, B.E. Boor, Infant and adult inhalation exposure to resuspended biological particulate matter, Environ. Sci. Technol. 52 (1) (2018) 237–247, https://doi.org/10.1021/acs.est.7b04183.
[66] D. Hospodsky, N. Yamamoto, W.W. Nazaroff, D. Miller, S. Gorthala, J. Peccia, Characterizing airborne fungal and bacterial concentrations and emission rates in six occupied children's classrooms, Indoor Air 25 (6) (2015) 641–652, https://doi.org/10.1111/ina.12172.
[67] S. Bhangar, J.A. Huffman, W.W. Nazaroff, Size-resolved fluorescent biological aerosol particle concentrations and occupant emissions in a university classroom, Indoor Air 24 (6) (2014) 604–617, https://doi.org/10.1111/ina.12111.
[68] S. Bhangar, R.I. Adams, W. Pasut, J.A. Huffman, E.A. Arens, J.W. Taylor, T. D. Bruns, W.W. Nazaroff, Chamber bioaerosol study: human emissions of size-resolved fluorescent biological aerosol particles, Indoor Air 26 (2) (2016) 193–206, https://doi.org/10.1111/ina.12195.
[69] S.S. Patra, T. Wu, N.D. Wagner, J. Jiang, E.B. Boor, Real-time measurements of fluorescent aerosol particles in a living laboratory office under variable human occupancy and ventilation conditions, Build. Environ. 205 (2021), 108249, https://doi.org/10.1016/j.buildenv.2021.108249.
[70] S. Bhangar, B. Brooks, B. Firek, D. Licina, X. Tang, M.J. Morowitz, J.F. Banfield, W. W. Nazaroff, Pilot study of sources and concentrations of size-resolved airborne particles in a neonatal intensive care, Unit. Build. Environ. 106 (2016) 10–19, https://doi.org/10.1016/j.buildenv.2016.06.020.
[71] P.S.J. Lakey, Y. Won, D. Shaw, F.F. Østerstrøm, J. Mattila, E. Reidy, B. Bottorff, C. Rosales, C. Wang, L. Ampollini, S. Zhou, A. Novoselac, T.F. Kahan, P.F. DeCarlo, J.P.D. Abbatt, P.S. Stevens, D.K. Farmer, N. Carslaw, D. Rim, M. Shiraiwa, Spatial and temporal scales of variability for indoor air constituents, Commun. Chem. 4 (1) (2021 12) 110, https://doi.org/10.1038/s42004-021-00548-5.
[72] P. Taimisto, M. Tainio, N. Karvosenoja, K. Kupiainen, P. Porvari, A. Karppinen, L. Kangas, J. Kukkonen, J. Tuomisto, Evaluation of intake fractions for different subpopulations due to primary fine particulate matter ($PM_{2.5}$) emitted from domestic wood combustion and traffic in Finland, Air Qual. Atmos. Health 4 (2011) 199–209, https://doi.org/10.1007/s11869-011-0138-3.
[73] J. Zhao, W. Birmili, T. Hussein, B. Wehner, A. Wiedensohler, Particle number emission rates of aerosol sources in 40 German households and their contributions to ultrafine and fine particle exposure, Indoor Air 31 (3) (2021) 818–831, https://doi.org/10.1111/ina.12773.

Update

Building and Environment

Volume 247, Issue , 1 January 2024, Page

DOI: https://doi.org/10.1016/j.buildenv.2023.111026

Building and Environment 247 (2024) 111026

Contents lists available at ScienceDirect

Building and Environment

journal homepage: www.elsevier.com/locate/buildenv

Corrigendum to "Size-resolved inhalation intake fractions for particles released from human activities in residential indoor environments" [Build. Environ. 244 (2023) 110763]

Dusan Licina [a,*], Brandon E. Boor [b,c]

[a] Human-Oriented Built Environment Lab, School of Architecture, Civil and Environmental Engineering, Ecole Polytechnique Federale de Lausanne (EPFL), Switzerland
[b] Lyles School of Civil Engineering, Purdue University, West Lafayette, IN, USA
[c] Ray W. Herrick Laboratories, Center for High Performance Buildings, Purdue University, West Lafayette, IN, USA

The authors regret to inform the editorial office about the error identified in Fig. 5 of the manuscript. Below, we provide the corrected Figure 5.

The figure caption remains identical.

The authors would like to apologise for any inconvenience caused.

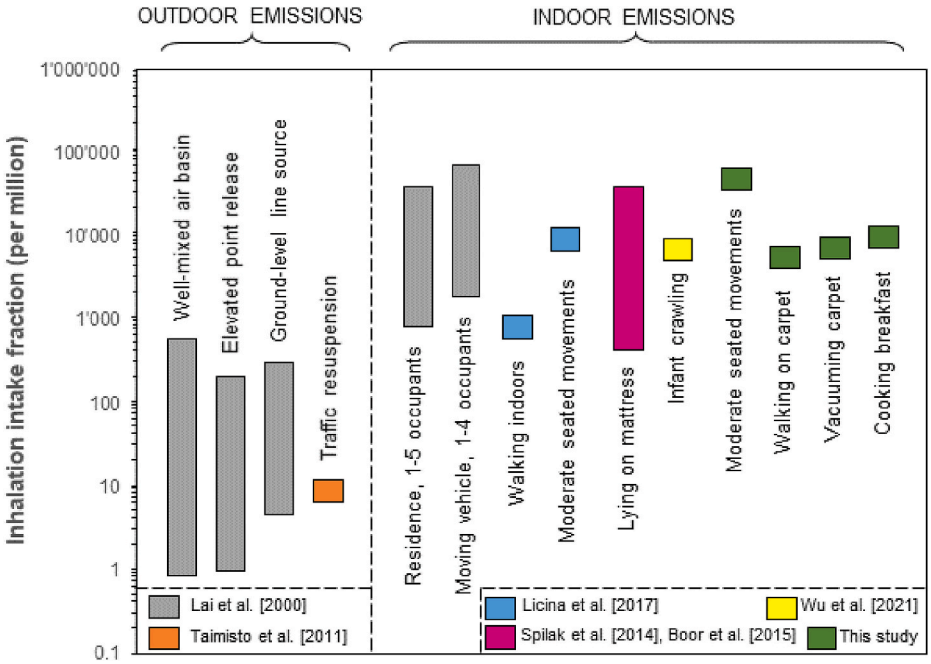

Fig. 5. Summary of ranges in inhalation intake fractions (per million, ppm) reported for (left) outdoor emission sources, including a well-mixed air basin, elevated point release, ground-level line source (Lai et al. [37]), and traffic-induced particle resuspension (Taimisto et al. [72]) and (right) indoor emission sources, including: residence, 1–5 occupants, interior of a moving vehicle, 1–4 occupants (Lai et al. [37]), walking indoors, moderate seated movements (Licina et al. [45]), mattress dust resuspension (1–5 μm and 5–20 μm size fractions) (Spilak et al. [26]; Boor et al. [21]), infant crawling-induced floor dust resuspension (Wu et al. [27]), and the four scripted activities evaluated in this study: moderate seated movements, walking on carpet, vacuuming carpet, and cooking breakfast. Modelling data are shown in gray color. (For interpretation of the references to color in this figure legend, the reader is referred to the Web version of this article.)

DOI of original article: https://doi.org/10.1016/j.buildenv.2023.110763.
* Corresponding author.
E-mail address: dusan.licina@epfl.ch (D. Licina).

https://doi.org/10.1016/j.buildenv.2023.111026

Available online 16 November 2023